

A Stochastic Object Model Conditioned to High-Quality Seismic Data

Anne Randi Syversveen · Ragnar Hauge ·
Jan Inge Tollefsrud · Ulf Læg Reid ·
Alister MacDonald

Received: 11 October 2010 / Accepted: 8 July 2011 / Published online: 8 October 2011
© The Author(s) 2011. This article is published with open access at Springerlink.com

Abstract We present an approach for modeling facies bodies in which a highly constrained stochastic object model is used to integrate detailed seismic interpretation of the reservoir's sedimentological architecture directly in a three-dimensional reservoir model. The approach fills the gap between the use of seismic data in a true deterministic sense, in which the facies body top and base are resolved and mapped directly, and stochastic methods in which the relationship between seismic attributes and facies is defined by conditional probabilities. The lateral geometry of the facies bodies is controlled by seismic interpretations on horizon slices or by direct body extraction, whereas facies body thickness and cross-sectional shape are defined by a mixture of seismic data, well data, and user defined object shapes. The stochastic terms in the model are used to incorporate local geometric variability, which is used to increase the geological realism of the facies bodies and allow for correct, flexible well conditioning. The result is a set of three-dimensional facies bodies that are constrained to the seismic interpretations and well data. Each body is defined as a parametric object that includes information such as location of the body axis, depositional direction, axis-to-margin normals, and external body geometry. The parametric information is useful for defining geologically realistic intrabody petrophysical trends and for controlling connectivity between stacked facies bodies.

A.R. Syversveen (✉) · R. Hauge
Norwegian Computing Center, P.O. Box 114, 0314 Blindern, Oslo, Norway
e-mail: anner@nr.no

J.I. Tollefsrud
Statoil, 0246 Oslo, Norway

U. Læg Reid
Bayerngas Norway AS, Lilleakerveien 8, 0283 Oslo, Norway

A. MacDonald
Roxar Software Solutions AS, Lysaker Torg 45, 1366 Lysaker, Norway

Keywords Facies modeling · Seismic data · Intrabody petrophysical trends

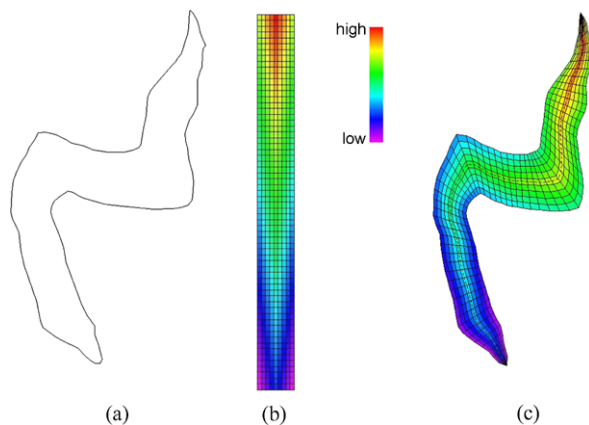
1 Introduction

Conventional seismic interpretation involves interpretation of stratigraphic horizons and faults in vertical cross sections. With increasing quality and resolution, seismic data can also be used to interpret facies architecture in map view. The interpretation in map view is generally based on using horizon slices that are aligned parallel to geological time lines. Interpreted facies elements, including turbidite channels and a variety of bars and lobes, have been used very successfully for well targeting in many significant discoveries during the last decade or so, and have also been integrated in static three-dimensional models used for development planning and reservoir management. Integration of seismic interpretation in a three-dimensional reservoir grid is straightforward for thick, well-resolved facies bodies, but can be more challenging for thinner facies bodies.

Where seismic quality is high, it is often possible to interpret sedimentological features on horizon slices also in places where the facies bodies are thinner than the seismic resolution. Although the tops and bases of the bodies cannot be resolved independently from the seismic data, the total seismic response, including interference effects, often produces a pattern that clearly responds to the facies architecture. The patterns seen on horizon slices can then be interpreted in terms of facies architecture. The approach described in this paper aims at providing a methodology that enables integration of these facies interpretations in three-dimensional reservoir models. The facies model is used as input to the petrophysical model, which again is used as input for flow studies.

Our approach is based on using a stochastic object model (Deutsch and Wang 1996; Holden et al. 1998) to represent facies as objects with a geometry that is highly constrained from the seismic interpretations. The parameters of the object model are primarily used to control thickness and shape of cross sections. In general terms, the seismic interpretation defines the facies shape in map view and the parameters of the object model control the shape in cross-section. As will be shown later, seismic and well data can also be used to constrain thicknesses. The stochastic terms in the model are used to incorporate local geometric variability from the idealized object model shapes to increase the geological realism of the facies architecture and allow for correct, flexible well conditioning. Object models can be conditioned to a variety of data types including well and seismic data. Conditioning to seismic data is usually done by establishing conditional probability functions that define the probability of finding a particular facies type given the seismic value; see Skare et al. (1996). Conditional probability functions can then be used to transform seismic attribute cubes into facies probability cubes, which are used to constrain stochastic facies simulation. This approach proposes objects independent of facies probabilities, and uses an accept/reject step to keep the good matches. It works nicely for a smooth probability cube, for which the seismic data define general facies volume fraction trends, but is useless if the facies geometries can be seen directly from the seismic data. In these cases, another approach for conditioning object models is to use the seismic data directly

Fig. 1 Illustration of parameterization and intrabody trends. (a) A polygon. (b) A petrophysical property is sampled on a regular grid. (c) The petrophysical property is mapped cell by cell to the polygon object



in the parameterization of the objects. Examples are given in Rabelo et al. (2007) for point bars and Viseur et al. (2001) for channels.

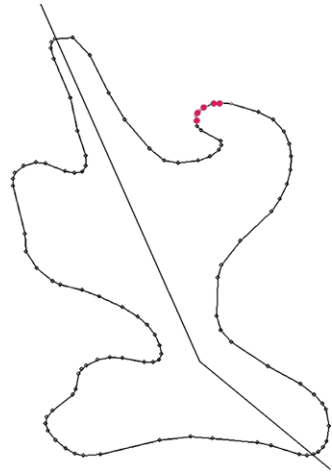
In this paper, we will instead use facies boundary polygons derived from seismic interpretations in the parameterization of the object model. The polygons are assumed as given, and hence we do not focus on how to extract them. Facies objects are then generated with edges and pinchout lines defined directly by the seismically interpreted polygons. The thickness profiles and the depth location of the object can be modeled using stochastic methods, and hence prior distributions for these parameters must be specified. The thickness can be conditioned to a thickness map extracted from the seismic data, or alternatively, the top and base of the object may be given as maps. The method will still give a parameterization of the body, as opposed to only a volume of cells. An advantage of this method compared to deterministic and pixel-based approaches is that the parametric representation allows for petrophysical trend modeling. This is illustrated in Fig. 1. With a parametric representation of the polygon, a petrophysical property sampled on a regular grid can easily be mapped to the polygon object; see also Hauge et al. (2003). The parametric shape is also useful for mapping thickness trends across and along the body, as in Lia et al. (1996).

2 Object Parameterization

Figure 1 illustrates both the horizontal parameterization of our object and the advantage of using an object. Although the geometry of the body is defined from the seismic data, the use of an object to define this geometry enables intrabody petrophysical modeling on a grid that conforms to the object. Stochastic property modeling on such an object-conforming grid can improve the geological realism, even without the intrabody trends illustrated in Fig. 1, by producing porosity and permeability anisotropy following the body geometry.

Our objects are parameterized horizontally along a piecewise linear curve representing the local x -axis for $y = 0$ and with the direction of the local axis defined at the endpoints of the linear segments as seen in Fig. 1. At regularly spaced locations,

Fig. 2 Branching object that cannot be parameterized. From the *red points*, it is impossible to draw a line to the other edge so that the line is inside the polygon



the distance to the edge is measured along the local y -axis. This object is closely related to the one used in Hauge et al. (2006), but the local y -axis is more flexible here, allowing for a greater range of objects. Although it is desirable that the local y -axis is perpendicular to the reference line, there is a tradeoff between this and being able to have wide and turning objects. If we look at Fig. 1 again, we see that the y -axes of the object start reacting to the turn before it occurs. If we do not do that, the local y -axes would intersect before we reached the edge of the object in the inside turn. This will give problems when going from a local to a global coordinate system because there will be no one-to-one correspondence between the two coordinate systems. We will come back to the parameterization in the next section.

Vertically, we add a top and bottom surface to the object. These surfaces have uncertainty in the form of two-dimensional Gaussian fields that enable well conditioning, following the approach in Lia et al. (1996) and Hauge et al. (2006). The difference is that the surfaces there were the product of independent one-dimensional curves along and across the object, whereas here we use full two-dimensional surfaces.

2.1 Generating the Horizontal Body Shape

Horizontally, the challenge is to define the internal grid shown to the right in Fig. 1, relying only on the outline being the polygon shown to the left. That is, we need to define the piecewise linear reference line and the local y -axes along this line. First, observe that we are not able to parameterize all kinds of polygon using this approach. For polygons that are branching, as shown in Fig. 2, it is impossible to define a legal set of y -axes. The condition for a polygon to be valid is as follows: For a definition of right and left edge, it must be possible to draw a line from any point on one edge to some point on the other edge so that the line is inside the polygon and does not intersect any other such line. The final y -axes we use for the object is one solution of this. There can be many such solutions, with different right and left edges and different y -axes, but as long as at least one such solution exists, the polygon can be parameterized using our approach.

Fig. 3 (a) A valid edge definition. (b) An invalid edge definition. *Right edge is red and left edge is blue. The black line is the reference line*

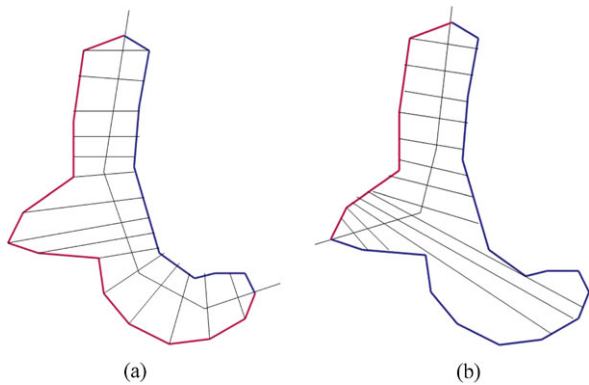
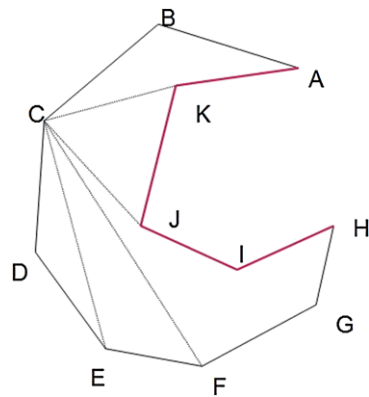


Fig. 4 Graph used to find *left* and *right* edge. The *dashed lines* are possible ways to go directly from point C. Similar paths are made for all other points. The two points furthest apart are A and H, and the shortest way goes via K, J and I



Whether a polygon is valid or not may depend on the choice of right and left edge, e.g. as shown in Fig. 3, where the polygon is valid when using the edge definition on the left, but not with the one on the right, for which we cannot draw a line from the points furthest to the right to the red edge without crossing the polygon. We do not take this into consideration when trying to parameterize a polygon. Instead, we define the right and left edges as separated by the two points that are furthest apart when measuring the distance inside the polygon. We approximate this distance by creating a graph. Each polygon point is a node in the graph, and there is an edge between two nodes if a straight line between the corresponding polygon points lies completely inside the polygon (Fig. 4). The weight of each edge is the length of the corresponding line, and we can find the distances between any two points by using Dijkstra’s algorithm; see Dijkstra (1959). This generally works well as long as it is natural for the reference line to start and end at a polygon point.

With the edges defined, the next step is to find a set of valid *y*-axes that moves reasonably straight across the object, and set the reference line to the center of these. This is visually simple, but requires a rather technical algorithm, which is given in Appendix. The key step is to define a temporary curve to give an idea of the local *x*-direction, and use this as a guide to where we want the local *y*-axes to go. This is

then conditioned to the requirement that y -axes should not intersect with each other before they have intersected with the polygon.

Instead of automatically generating the reference line, it is possible to control this by a piecewise linear trend line defined by the user. This line will be used to define the right and left edge, with the two polygon points furthest apart along this line as the dividing points. Furthermore, we use normality to this line as our ideal y -axis direction. We then generate the final y -axes as before.

2.2 Generating the Vertical Body Shape

With the horizontal parameterization in place, the vertical body shape is given by the top and bottom surfaces. There are three options for how to specify these surfaces depending on what can be seen in the seismic data:

1. Top and bottom surface given as a general shape, when they cannot be seen from the seismic data. In this case, the global thickness of the object and the depth location must be given by prior distributions (Fig. 5a).
2. Thickness is mapped from the seismic data, but the distribution of the thickness above and below the plane is given as a general trend. Here, the global thickness is specified, but the depth location must be defined by a prior distribution (Fig. 5b).
3. Both top and bottom surface are mapped from the seismic data. This gives both global object thickness and location in depth (Fig. 5c).

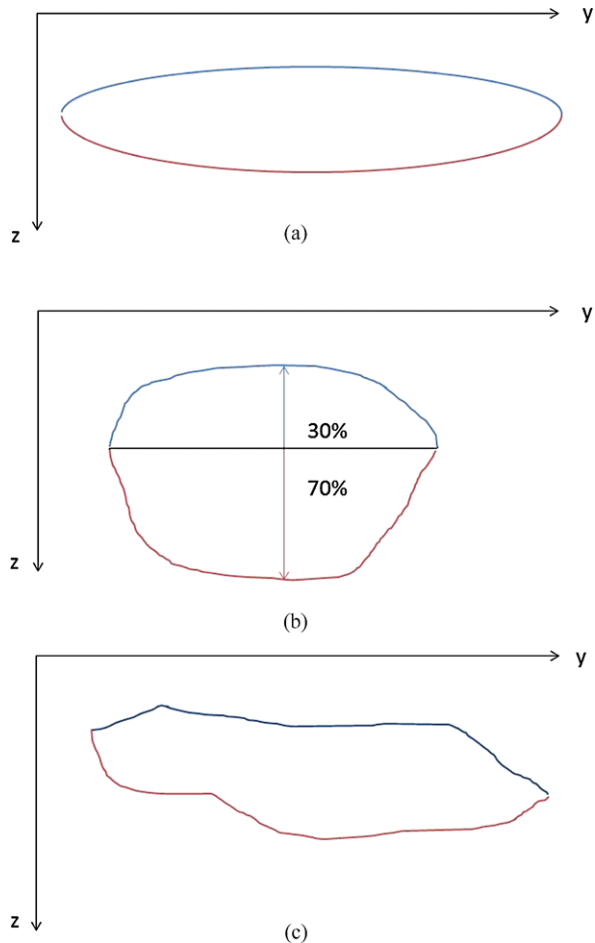
Again, we do not concern ourselves with how these maps are created from the seismic data; we use them as input data for our model. For the full three-dimensional body, the parameterized polygon will be the outline of the body when projected into the xy -plane. We now have the trend shape for the top and bottom of the object, and add Gaussian random fields to give the final complete shape. These fields have the trend as expectation, and relatively small standard deviations. They are there to give a smooth random variation in the body. These local deviations make it much easier to match well observations, particularly when an object passes through several wells; see Syversveen and Omre (1997).

2.3 Generating Objects from Invalid Polygons

The top and bottom surfaces can be utilized to parameterize polygons that are not valid in the sense defined above; that is, polygons for which no set of y -axes going from edge to edge without intersecting is found. Observe that all convex polygons are trivially valid. This means that we can make a local convex closure in the problematic area, and set the top and bottom equal in the area that is outside the original polygon, but inside the new closure. The local convex closure is a straight line between two points on the polygon that lie entirely outside the polygon (Fig. 6). The final object will have zero thickness in this area. Trends and anisotropy in intrabody modeling will be relative to the extended polygon, giving a behavior as if the zero-thickness area has been eroded away.

The algorithm for generating objects from invalid polygons is as follows:

Fig. 5 The three alternative ways to model thickness of objects. **(a)** No seismic thickness information. User specified top and bottom profile along and across object. **(b)** Thickness given from seismic data. User specifies percentage of thickness above and below reference plane. **(c)** Both top and bottom of object are given from seismic data



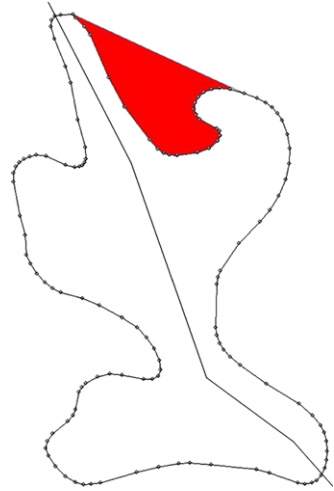
1. Identify a point from which no legal y -axis can be drawn.
2. Find a possible local convex closure in the vicinity of this point.
3. Implement this closure, and proceed to Step 1 until no further problems are detected.
4. Remove unnecessary closures. These can be found since no y -axis in the closure interval intersects the original polygon more than twice (once for each edge).

This approach is useful if the closures are small and/or irrelevant for the modeling (they mainly interfere with trends across the body). It is, of course, also useful if erosion is actually a relevant explanation for the invalidity of the original polygon.

2.4 Adding Uncertainty to the Horizontal Edges

If the horizontal outline of the body is not seen clearly, three polygons may be given instead of one, representing the maximum, the mean and the minimum of the body. First, we use the algorithm described above on the maximum polygon. Then, we

Fig. 6 Local convex closure of a branching polygon. The final object will have zero thickness in the *red area*



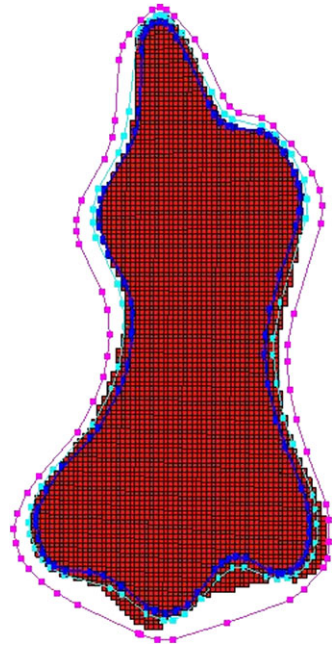
associate the mean polygon with zero in a standard Gaussian distribution and the maximum and minimum with a user-specified number of standard deviations. Mainly, the idea is to draw a one-dimensional standard Gaussian field and map it to a location between the polygons. Zero is the mean, negative values go toward the minimum and positive values toward the maximum. The minimum and maximum polygons truncate the value, so values beyond the given number of standard deviations will result in following the minimum or maximum polygon locally there. The range of the Gaussian fields controls the smoothness of the objects. A point on the left edge can be correlated with the corresponding point on the right edge, and this correlation controls how well the edges will follow each other.

The detailed algorithm is as follows:

1. Let a be the number of standard deviations associated with minimum or maximum.
2. Draw two numbers x_1 and x_2 , one for each end of the object, from a standard normal distribution.
3. Use these points to find the length of the object:
 - a. If x is greater than a , use the maximum polygon at this end.
 - b. If x is between 0 and a , map to the point that lies x/a of the way between the mean and the maximum.
 - c. If x is negative, do a similar mapping between the mean and minimum.
4. Draw two one-dimensional Gaussian fields, one for the left edge, and one for the right.
5. Do a similar mapping for each sample of the edges.

An example is shown in Fig. 7. When conditioning on wells, the Gaussian fields are conditioned to include or exclude well positions depending on whether the object should match them or not.

Fig. 7 Object with uncertainty on horizontal edges. The object is shown in *red*; the *pink*, *turquoise* and *blue lines* show the maximum, expected and minimum polygon



3 Well Conditioning

We use standard object model methods for well conditioning; see Syversveen and Omre (1997) and Hauge et al. (2007). The idea is to first condition global parameters to the well data and then let the edge uncertainty and two-dimensional top and bottom uncertainty fields handle the detailed match. We start by scanning through a discretized set of possible depth locations. At each depth, we find well intersections and see if these are of a facies that we may condition upon or pass through as a locally eroded object (the facies seen in the well erodes the object facies). At each location, we compute the likelihood for creating an object that matches the wells at that depth. This likelihood contains the likelihood for the top and bottom surfaces, and if the thickness follows a priori, the likelihood for this is included as well. This likelihood is multiplied by the prior likelihood for having the object at this depth. Even in the case with given top and bottom surfaces, we set an uncertainty on the depth and follow this procedure. If the surfaces are inconsistent with well observations, we still get a realization that fulfills well conditioning, but the top and bottom surfaces will not be reproduced at well locations.

A depth value is drawn from the normalized likelihoods that define a distribution for depths. The object is then created conditional to the well observations at this depth, avoiding illegal observations by using edge uncertainty, and passing through wells either by conditioning or as eroded. A conditioning intensity parameter is used to define a bonus the object will receive for conditioning observations. If intensity is set high, the object will try to condition as many observations as possible while keeping the shape defined by the model. This can give undesirable results, since all

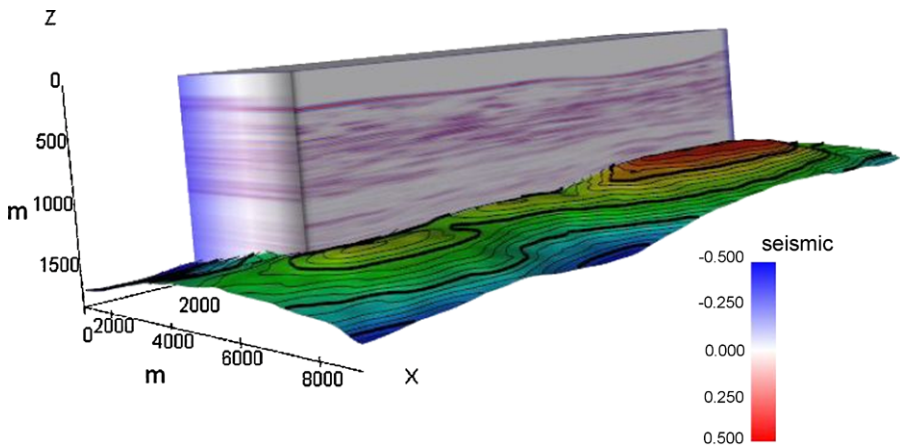


Fig. 8 Seismic cube shown with base reservoir map

prior distributions are more or less ignored, giving large flexibilities in depth and uncertainty of top and bottom. With a more modest setting, the object will condition observations that fit the specified shape reasonably well, but avoid observations that are too narrow and pass eroded through those that are too wide. In general, how to set the intensity parameter should depend on the number of bodies assumed to be in a full model. If this object is the only one that can fit the well observations, it should be high, in order to ensure that all observations are covered. The more bodies that could fit the observations, the more relaxed the setting should be. The final result should be checked, considering whether the polygon body covers a reasonable number of observations compared to its size, well density and the number of other objects that might have covered these observations.

Instead of trusting this auto detection of suitable observations, the user may also specify a set of observations that the object must condition. This information is then used when drawing depth, and if applicable, thickness, and the two-dimensional fields will ensure matching with these observations. The algorithm handles any number of wells, and will always give a valid object unless there is an explicit conflict between the defined object and the well data, for example, if a vertical well inside the minimum polygon contains only shale, and we are modeling sand objects.

4 Case Study

The case study is based on a deep-water turbidite slope deposit. The seismic (Fig. 8) and well data presented are synthetic. The seismic data indicate the presence of turbidite slope sands. Intra-body petrophysical trends are important for turbidite bodies, because grain size differs along and across bodies, so our method is well suited. Six potential reservoir bodies have been interpreted from the seismic data; see Fig. 9. The thicknesses of the bodies are close to or lower than the seismic resolution. We will see examples of the three different thickness and depth models mentioned above. Three

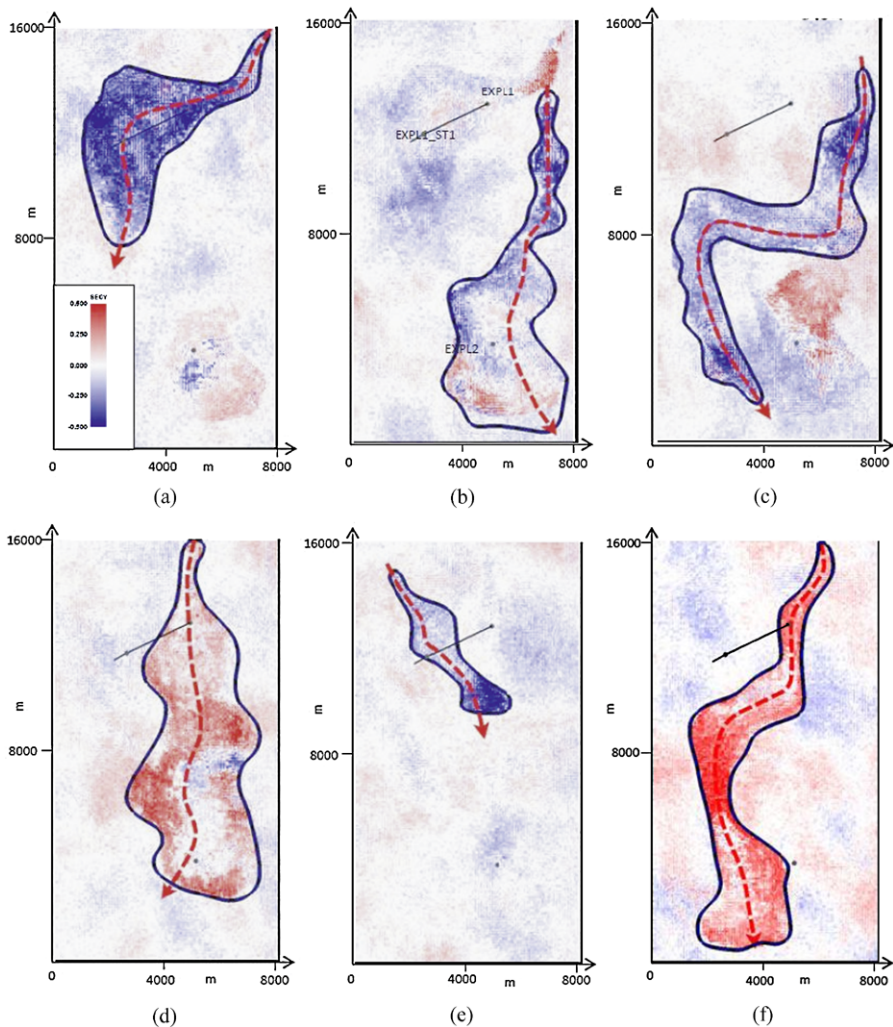


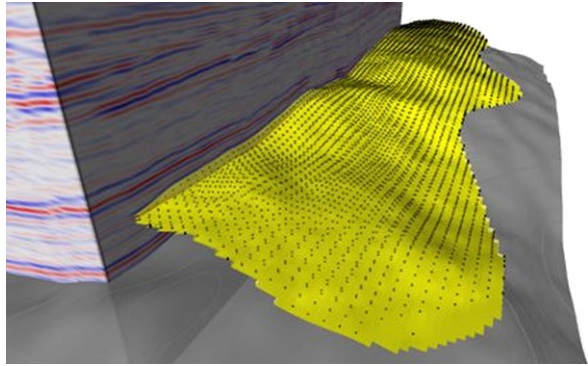
Fig. 9 Polygon and trend line (*dashed red line*) of Body 1 to Body 6 displayed with acoustic impedance at different depths. The *black dots and line* are wells

synthetic exploration wells have been drilled based on the body interpretations. The exploration wells support the presence of turbidite sand bodies.

4.1 Seismic Information

The information we can extract from the seismic data differs for the different objects and depends on the resolution of the seismic wavelet, as well as on the contrast between the different facies associations within the zone of interest. For all objects, we have interpreted a polygon describing the outer limit of the body from the seismic data. The polygons for all six bodies can be seen in Fig. 9. A trend line has also been

Fig. 10 Main body (Body 4) shown with extracted points and top and base map defining the volume



interpreted for each body. This line describes where to expect the thickest area of the bodies. The petrophysical trend will also follow this line. The trend lines are shown as dashed lines in Fig. 9.

Some objects are interpreted as very thin (in the range of 10–20 meters), whereas others range from 10–40 meters in thickness. The main sand body in the reservoir is well defined, and its thickness has been interpreted to be at a maximum of around 50 meters. Because of this difference in response, we have used different interpreted input data when simulating the bodies. The thicker, main body has been easily mapped by geo-body extraction (Fig. 10), whereas the thickness of the intermediate objects is described by a thickness map derived from seismic response. The thinner, less defined bodies are described by an expected thickness based on well observations and interpretations.

4.2 Well Data

All observed objects have been conditioned to wells. Some wells have several observations, and we can assign one of the observations to an object by specifying the prior distribution for depth accordingly. From the seismic data (Fig. 9), we can also see that Body 1 and Body 4 can possibly have observations in more than one well; see the black dots. Well logs are shown in Fig. 11. Observations at same stratigraphical level have been conditioned to the same object (Fig. 11/Fig. 12). By correlating observations, we ensure that the object will exist at these locations after simulation.

4.3 Facies Bodies and Three-Dimensional Model

The resulting model can be seen in Fig. 13, where the bodies are coded by a discrete index. Figures 14 to 16 show the resulting body thickness of three of the turbidite bodies. These have all been modeled using different thickness distributions. Figure 14 shows Body 1, which is one of the thinner bodies. The (global) thickness is drawn from a normal distribution with an expected value of 17 meters. Body 2, shown in Fig. 15, is of intermediate thickness, and its thickness distribution is described by a thickness map. The difference in maximum thickness between the input and the result is due to variability added to the thickness map. For Body 4, shown in Fig. 16, a top and a base map have been used as input. This is the thickest body that is modeled.

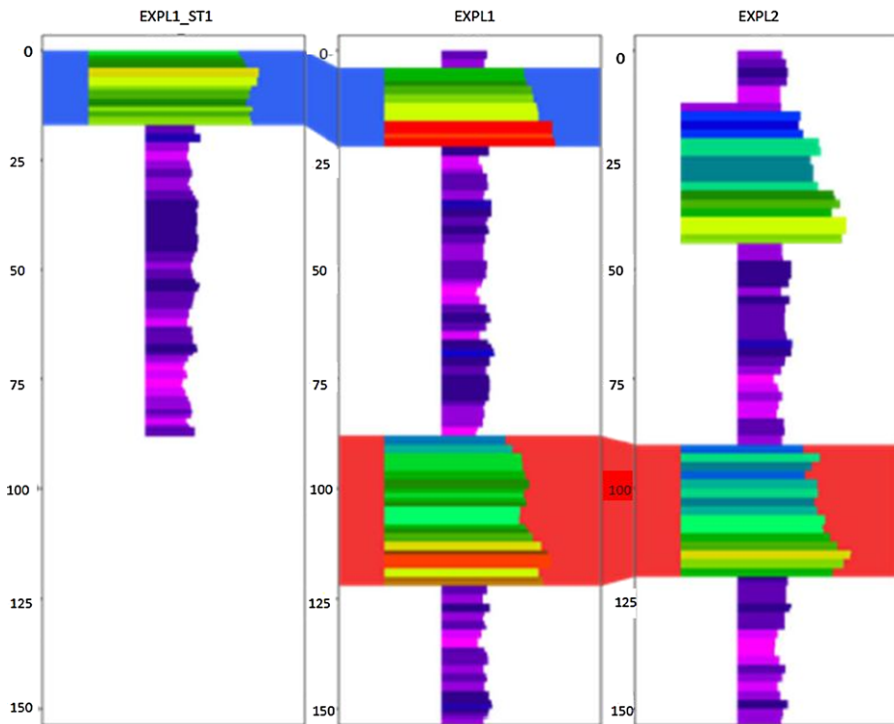


Fig. 11 Correlation of Body 1 in well EXPL1 and EXPL1_ST1 (*blue*) and correlation of Body 4 in well EXPL1 and EXPL2 (*red*). Both correlations are shown in stratigraphical simbox depth

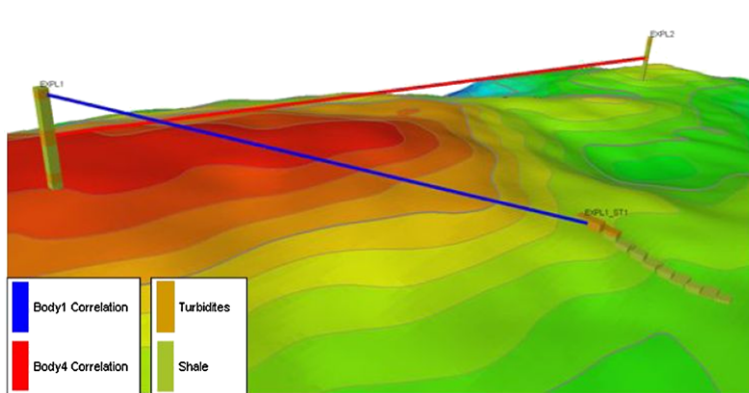


Fig. 12 Correlation of Body 1 in well EXPL1 and EXPL1_ST1, and of Body 4 in well EXPL1 and EXPL2

4.4 Petrophysical Modeling

The resulting facies model has been used as input for petrophysical modeling. The parametric representation of the bodies makes it possible to include intrabody trends in the petrophysical properties. Figure 17 shows the simulated porosity for all six

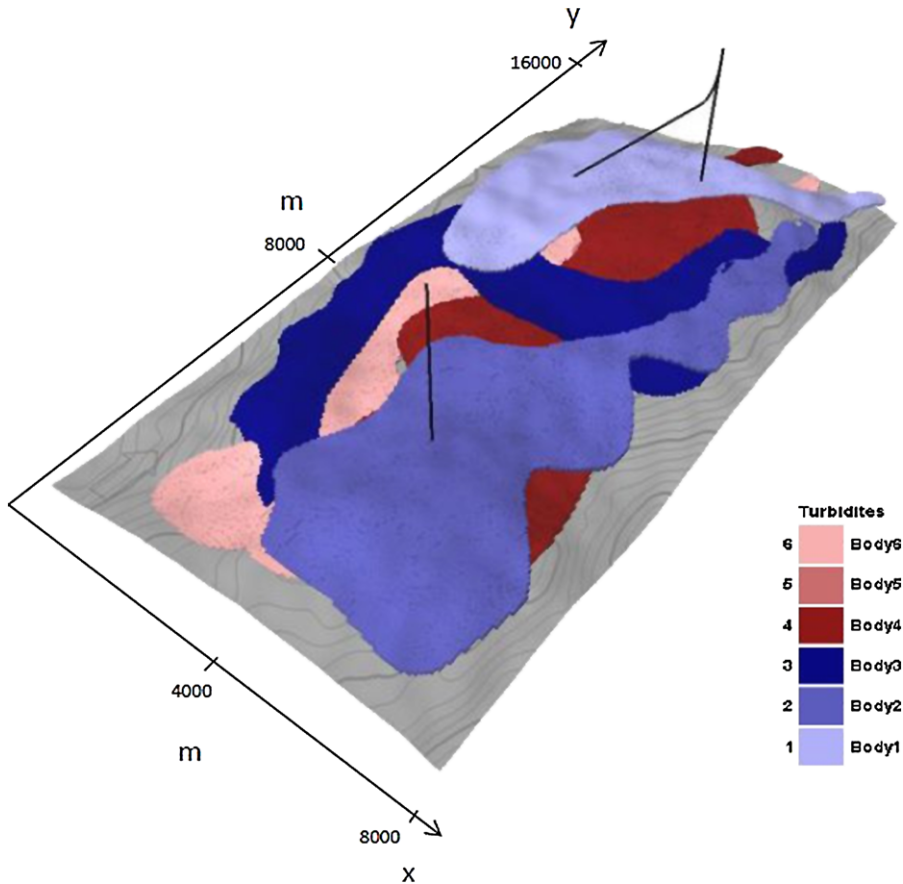


Fig. 13 Simulated bodies shown with discrete indexing

bodies, conditioned to well data. The porosity trend decreases from axis to margin, and from proximal to distal end of the object. Simulated porosity based on Body 4 is shown in Fig. 18.

5 Conclusions

We have presented a method for modeling objects seen in seismic data. Both information about lateral extent and thickness extracted from the seismic data can be taken into account. Objects are given a parameterization that enables intrabody modeling of petrophysical trends. Conditioning and correlation of any number of wells is also taken care of.

The method fills the gap between deterministic and stochastic facies modeling. When the seismic resolution is high, the uncertainty is low, and purely deterministic models can be used. When the seismic resolution is low, facies probability cubes can be extracted from the seismic data, and stochastic models can be conditioned to

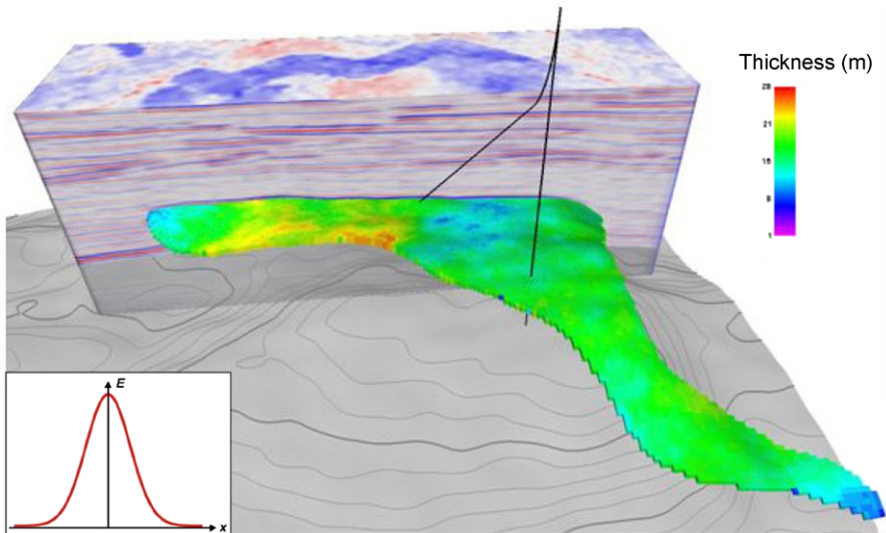


Fig. 14 Body 1 shown with the seismic on top of the base reservoir map

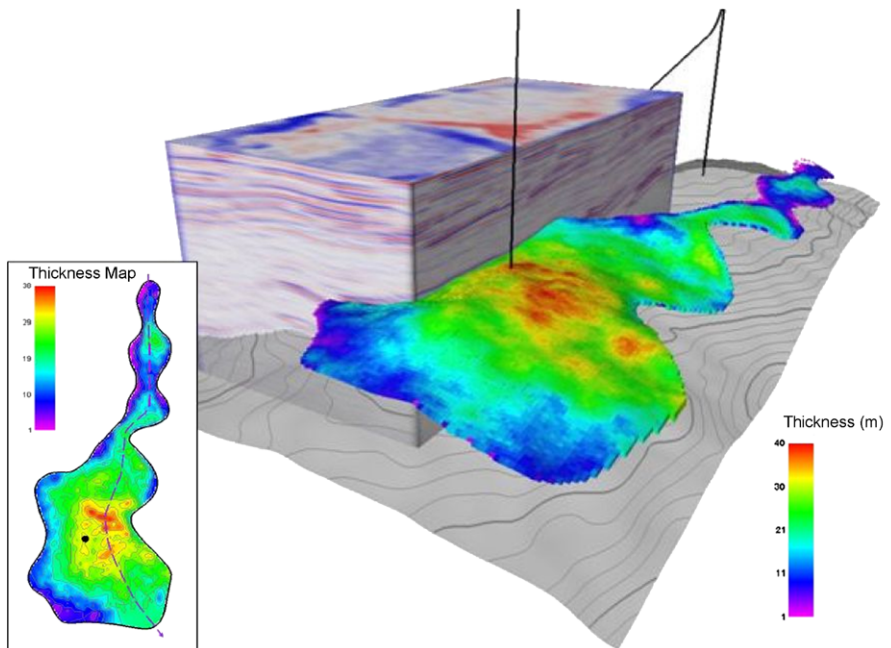


Fig. 15 Body 2 shown with the seismic on top of the base reservoir map

the facies probability cubes. Our approach works well when the seismic data are of intermediate quality, for example if the lateral extent of the object can be seen, but no information about depth and thickness is available. The stochastic model handles this

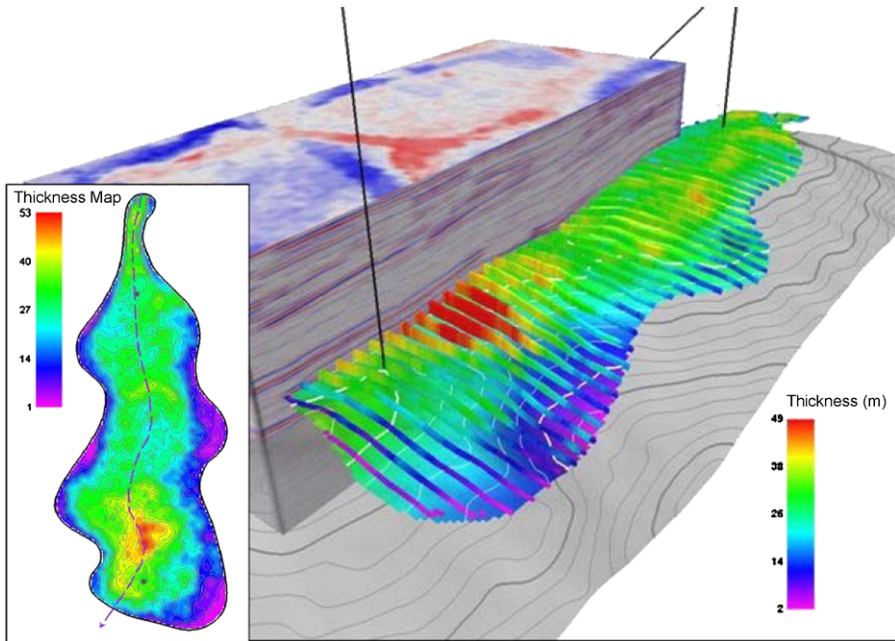


Fig. 16 Slices of Body 4 with body base map underneath. The thickness described by the body top/base map is shown to the left. The difference in maximum thickness is due to variability added to the body top/base map

uncertainty, and the parametric approach gives a realistic body shape when we add top and bottom. Even when a full body can be extracted from the seismic data, the method presented here has an advantage over pure pixel-based methods. By having internal body geometry, we can do intrabody modeling of petrophysical trends, and also get intrabody anisotropy when simulating petrophysical properties. This can be important for flow simulation.

The methodology has some limitations. First of all, it requires that we be able to draw a complete polygon from the seismic data, and not just a partial object. Furthermore, the parameterization limits the set of valid polygons to those with a well-defined left and right edge. The latter limitation can be overcome, but at the cost of no longer being able to use trends across the body in any meaningful manner.

Modeling of intrabody trends is important in turbidite deposits, because the grain size varies along and across the turbidites. We have demonstrated the use of our model on synthetic seismic data from a turbidite deposit. Six turbidite objects are simulated, conditioned to polygons and thickness maps extracted from the seismic and well data. The polygon shapes are recreated, and well conditioning is fulfilled. Our parametric approach allows the generation of intrabody porosity trends in objects.

Appendix: Algorithm for Defining Local x - and y -Axes in the Polygon

The polygon and the edges are given; the goal here is to find a parameterization that gives realistic intrabody behavior. This means finding the reference line, that is,

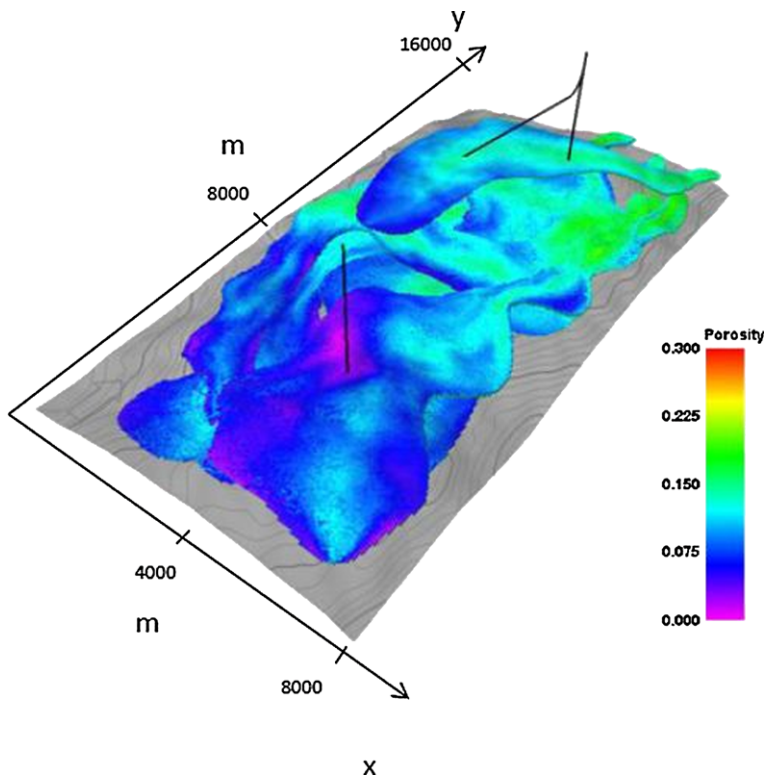


Fig. 17 Simulated porosity shown for all turbidite bodies. Note the intrabody trends (decreasing proximal to distal/axis to margin)

a central x -axis that runs centrally along the object, and local y -axes that are approximately perpendicular to this. Note that in the following, a point may be anywhere; if we mean on the polygon, we say polygon point.

1. Find legal intervals for each polygon point:
 - a. Find the points on the opposite edge that can be reached by a straight line from this point without leaving the polygon. This gives one or more intervals.
 - b. Truncate the intervals for explicitly pointwise legality:
 - i. When going from one end to the other, a polygon point cannot have a legal interval that extends further than the minimum end point of the intervals of all later polygon points. Remove such intervals.
 - ii. Similarly, a polygon point may not have a legal interval starting before the maximum start point of the intervals of all earlier polygon points. Remove such intervals.
 - c. To ensure that all points between the polygon points are also legally mapped, set the legal interval for a polygon point equal to the intersection of the legal interval for the polygon point and its closest neighbor to the left and right from point b. This ensures that all points between two polygon points can be legally mapped.

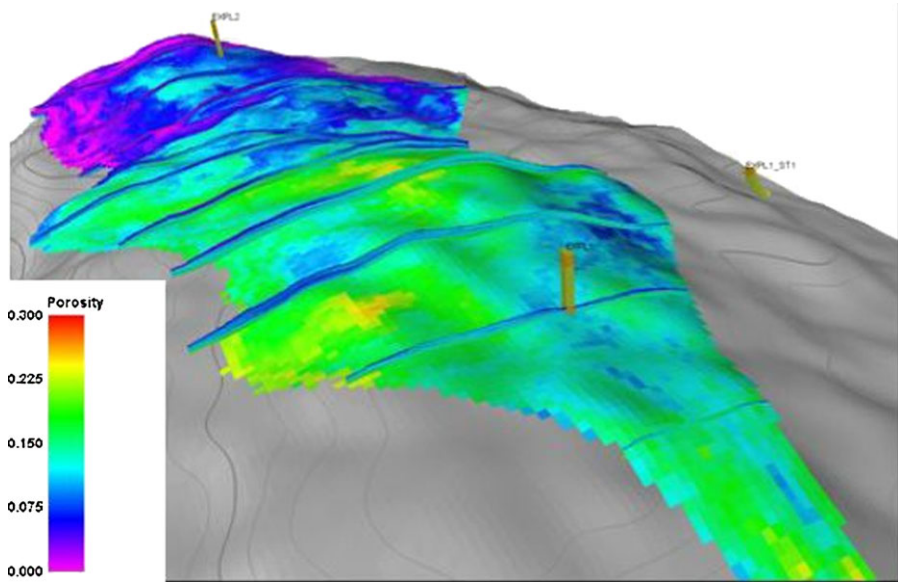


Fig. 18 Intrabody porosity of Body 4

2. Do the following for all polygon points on the right: For the first interval belonging to polygon point no i on right hand side, check that the polygon points on the left before this interval have an interval starting before i . If they do not, the polygon is invalid. Similarly, check the polygon points after the end of the last interval belonging to i . They should have an interval ending after i .
3. Check that all the polygon points still have valid intervals and that each polygon point is in a legal interval for another. If not, the polygon is invalid.
4. If a reference line is given, use this as a temporary x -axis.
5. Otherwise, find a temporary reference line (x -axis):
 - a. For each polygon point along each edge, find its relative position along the edge.
 - b. Draw a line to the same relative position on the opposite edge.
 - c. Let the center point of this line be a point on the temporary piecewise linear reference line.
6. At each point where there is a change of direction in the reference line, draw a line halving the angle between the neighboring pieces. At the edges, draw this line normally to the first and last piece. If these lines intersect before leaving the polygon, tilt them so that this no longer happens.
7. Move from one end of the polygon to the other:
 - a. Find the first unused polygon point on each edge.
 - b. Draw a line from each of these polygon points to the opposite edge. The ideal line will, when extended, pass through the intersection point of the lines in Step 5 at each edge of the piece. However, this line may not be legal due to the intervals from Step 1. In this case, move the end point the minimum distance possible to make the line legal.

- c. We have now defined two possible y -axes. If they do not intersect, use the one that comes first.
- d. If the possible y -axes intersect, resolve this by moving the end point for one of them so that it comes before the polygon point that the other starts at. If this is possible for both points, do it so that the lines are closest to the ideal.

This gives a set of valid y -axes. If such a local y -axis intersects its neighbors in the same point, or if it is parallel to both its neighboring axes, it is removed, since the interpolated local y -axis will give the same result. Finally, the piecewise linear x -axis is set as the curve going linearly between the midpoints of the remaining y -axes. This, together with the directions of the remaining y -axes, defines the horizontal parameterization.

Open Access This article is distributed under the terms of the Creative Commons Attribution Noncommercial License which permits any noncommercial use, distribution, and reproduction in any medium, provided the original author(s) and source are credited.

References

- Deutsch C, Wang L (1996) Hierarchical object based stochastic modeling of fluvial reservoirs. *Math Geol* 28:857–880
- Dijkstra EW (1959) A note on two problems in connexions with graphs. *Numer Math* 1:269–271
- Hauge R, Syversveen AR, MacDonald A (2003) SPE 84053 modeling facies bodies and petrophysical trends in turbidite reservoirs. Presented at SPE ATCE, Denver, Colorado, USA 2003
- Hauge R, Syversveen AR, MacDonald A (2006) Object models with vector steering. *Math Geol* 38(1):17–32
- Hauge R, Holden L, Syversveen AR (2007) Well conditioning in object models. *Math Geol* 39:383–398
- Holden L, Hauge R, Skare Ø, Skorstad A (1998) Modelling of fluvial reservoirs with object models. *Math Geol* 30:473–496
- Lia O, Tjelmeland H, Kjellesvik LE (1996) Modeling of facies architecture by marked point models. In: Baafi E, Schofield N (eds) *Geostatistics Wollongong '96*, vol 1. Kluwer Academic, Dordrecht, pp 386–387
- Rabelo IR, Luthi SM, van Vliet LJ (2007) Parameterization of meander-belt elements in high-resolution three-dimensional seismic data using the geotime cube and modern analogues. In: *Seismic geomorphology: applications to hydrocarbon exploration and production*. Special publications, vol 277. Geological Society, London, pp 121–137
- Skare Ø, Skorstad A, Hauge R, Holden L (1996) Conditioning a fluvial model on seismic data. In: Baafi E, Schofield N (eds) *Geostat Wollongong '96*, vol 1. Kluwer Academic, Dordrecht, pp 465–476
- Syversveen AR, Omre H (1997) Conditioning of marked point processes within a bayesian framework. *Scand J Stat* 24:341–352
- Viseur S, Shtuka A, Mallet J-L (2001) Stochastic object-based simulation of channels constrained by high resolution seismic data. In: *Proceedings from IAMG, Cancun, Mexico*